Accurate and Efficient Proximity Effect Correction for Electron Beam Lithography Based on Multilayer Perceptron Neural Network

Wenze Yao
College of Electrical and Information Engineering
Hunan University
Changsha, China
wenzeyao@hnu.edu.cn

Hongcheng Xu
College of Electrical and Information Engineering
Hunan University
Changsha, China
hongchengxu@hnu.edu.cn

Haojie Zhao
College of Electrical and Information Engineering
Hunan University
Changsha, China
haojie_zhao@hnu.edu.cn

Yujie Yang
College of Electrical and Information Engineering
Hunan University
Changsha, China
yujieyang2426@hnu.edu.cn

Siyuan Zhang
College of Electrical and Information Engineering
Hunan University
Changsha, China
siyuanzhang0103@hnu.edu.cn

Xin Zhang
College of Electrical and Information Engineering
Hunan University
Changsha, China
zhangxin2302@hnu.edu.cn

Jie Liu
College of Electrical and Information Engineering
Hunan University
Changsha, China
jie_liu@hnu.edu.cn

2022 International Workshop on Advanced Patterning Solutions (IWAPS) | 979-8-3503-9766-6/22/$31.00 ©2022 IEEE | DOI: 10.1109/IWAPS57146.2022.9972305

***Abstract*—This paper proposes a proximity effect correction (PEC) method for electron beam lithography (EBL) using multilayer perceptron (MLP) neural network (NN). By leveraging the symmetric characteristics of the point spread function (PSF), several annular regions divided around the exposure point are used as the input of NN. The exposure dose after traditional model-based PEC is used as the output when training NN. The PEC inference error of trained NN for grating with different periods can reach the same level as model-based PEC method (relative error is less than 1%). Meanwhile, the inference speed of the NN-based PEC is more than 7~10 times faster than that of the model-based PEC, which can significantly enhance the efficiency of PEC.**

Keywords—electron beam lithography, proximity effect correction, multilayer perceptron, neural network

I. INTRODUCTION

Electron beam lithography (EBL) is a high-resolution technique, which can manufacture the sub-10 nm precision device [1, 2]. The grating structure is a periodic pattern widely used in surface acoustic wave (SAW) devices [3], optical phased array [4], etc. However, the electron beam scattering in the resist and substrate seriously jeopardizes the fabrication quality, which is named the "proximity effect" (PE) [5]. As shown in Fig. 1, when exposing a small target region (blue area), the incident electrons are scattered and reflected by the resist/substrate, leading to undesirable exposure of a large region (orange and even green areas). The point spread function (PSF) is introduced to quantify the energy deposition distribution of this electron beam scattering. Therefore, proximity effect correction (PEC) is an extremely important step, especially for complex layouts at the nanoscale.

The mainstream model-based PEC methods [6, 7] are used to correct the pattern shape and incident dose of the exposure layout via iterative optimization. Although such methods can achieve high PEC accuracy, as the critical dimensions (CD) of EBL fabrication are further reduced, the computational cost of the model-based PEC rises sharply. In recent years, machine learning technology has prevailed in the field of lithography, which can avoid complex iterative operations. In the field of PEC, the unsupervised neural network (NN) [8] method result in a considerable improvement in speed. But for nano-sized CD nodes, the inference accuracy of the network is difficult to meet the design requirements. In [9, 10], MLP NN applied to the optical proximity correction (OPC), which has high OPC accuracy and efficiency, has an important impact on the study of PEC methods based on machine learning technology. Although MLP NN is mostly used in the OPC, similar methods have seldom been reported in PEC for EBL.

In this work, we propose an accurate and efficient PEC method based on the multilayer perceptron (MLP) NN. According to a specific EBL simulation condition, the MLP NN training samples are obtained through the traditional model-based PEC method. The input and output layers of NN are set in a given mode, and a convergent network model is constructed and trained. The trained model can directly infer the exposure dose after PEC, under the corresponding training EBL conditions. This method can effectively avoid the complex PEC iteration process, and thus improve the PEC calculation efficiency. In this article, we train MLP NN based on the grating structure to verify the effectiveness of the proposed method.

In section II, the PEC computation process and the MLP NN architecture training method are explained in detail; in section III, a series of layouts are used to quantitatively show the efficiency and accuracy of the proposed method; in section IV, we make a summary of this paper.

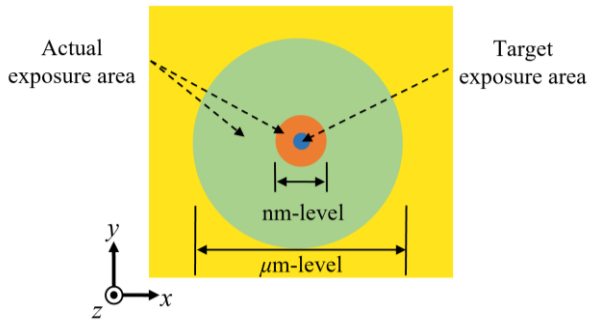

Fig. 1. Schematic diagram of the energy distribution of electron beam exposure.

II. MODEL AND METHOD

This section separately illustrates the traditional model-based PEC method, the proposed MLP NN architecture, and the NN training process.

A. Model-based PEC process

The scattering model of the electron beam on resist and substrate is mainly composed of forward scattering and back scattering. Without loss of generality, here the energy distribution curve of electron beam exposure is represented by a double Gaussian (2G) PSF [5]

$$P(r)=\frac{1}{\pi(1+\eta)}\left[\frac{1}{\alpha^2}\exp\left(-\frac{r^2}{\alpha^2}\right)+\frac{\eta}{\beta^2}\exp\left(-\frac{r^2}{\beta^2}\right)\right] \tag{1}$$

where α, β, and η representing the forward scattering range, back scattering range, and the ratio of forward scattering to back scattering energy density. And α, β, and η are determined by thicknesses and materials of resist and substrate, and can be computed using the Monte Carlo method [11].

The energy deposition density distribution after electron beam exposure is expressed by

$$E(\boldsymbol{r})=\sum_{i=1}^{N}P(|\boldsymbol{r}\text{-}\boldsymbol{r}_i|)\,D(\boldsymbol{r}_i)s^2 \tag{2}$$

where $E(\boldsymbol{r})$ is the energy deposition distribution at the pixel $\boldsymbol{r}$ and $D(\boldsymbol{r}_i)$ is the incident electron dose in the i^{th} mesh ($1\le i\le N$, and $i\in$Z); s is the actual side length of each mesh; N is the total number of pixels.

The mainstream PEC method is to obtain the uniform energy deposition $E(\boldsymbol{r})$ by adjusting the exposure dose $D(\boldsymbol{r}_i)$. In this paper, we construct training samples through an model-based PEC method [7], and we compare the accuracy and efficiency of the proposed method with this method (section III).

The threshold model is used to simulate the development process after electron beam exposure. The contour after development can be expressed as

$$\varphi(\boldsymbol{r})=\begin{cases}0, E(\boldsymbol{r})<\tau\\ 1, E(\boldsymbol{r})\ge\tau\end{cases} \tag{3}$$

where τ is the development threshold; $\varphi(\boldsymbol{r})$ is the developing contour function at the pixel $\boldsymbol{r}$. When the energy deposition of the exposure pixel is greater than the development threshold, it is regarded as complete development; otherwise, it is regarded as undeveloped. The error after development is defined as

$$\text{Error}=\frac{\sum_{i=1}^{N}|\varphi(\boldsymbol{r}_i)\text{-}T(\boldsymbol{r}_i)|^2}{N} \tag{4}$$

where $\varphi(\boldsymbol{r}_i)$ and $T(\boldsymbol{r}_i)$ are the development matrix and the target layout matrix, respectively.

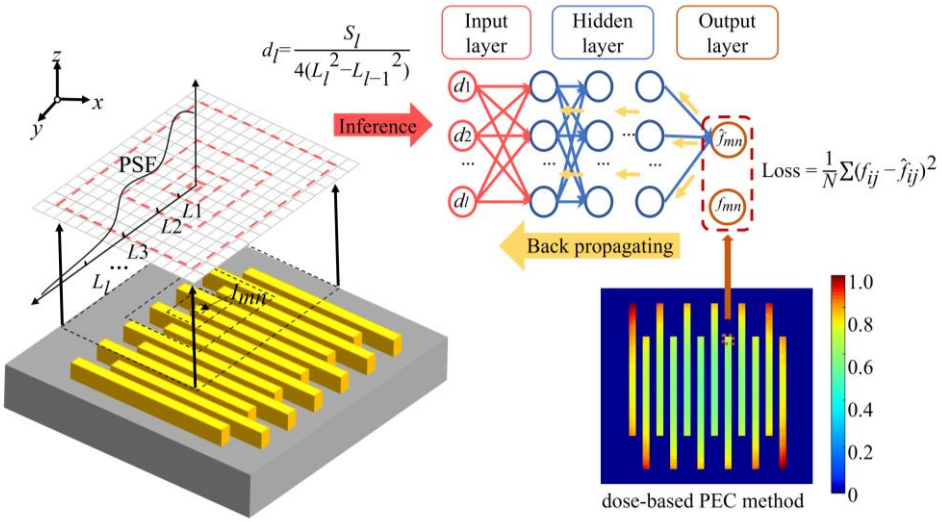

Fig. 2. The architecture of the proposed PEC method by MLP NN which includes obtaining input layer parameters by PSF, inference process, backpropagation method, etc.

B. MLP NN architecture

The MLP NN architecture includes three parts: an input layer, the hidden layers, and an output layer as shown in Fig. 2. For each pixel in the layout I_{mn} ($1<m<M$, $1<n<N$, M and N are the length and width of the layout matrix, respectively), we use L_1, L_2, ..., L_l ($l>2$) as the boundary to divide the PSF into l equal integral areas S_1, S_2, …, S_l, where the area integrals of l regions satisfy $S_1=S_2=\ldots=S_l$. The maximum PSF radius is set to 95% of the entire exposure energy. The layout exposure ratio in each ring area d_1, d_2, …, d_l is set as the MLP NN input neuron label

$$d_l=\frac{P_l}{4(L_l^2\text{-}L_{l\text{-}1}^2)} \tag{5}$$

where P_l is the exposed area in the ring-shaped area bounded by L_{l-1} to L_l.

For the j^{th} (j=1, 2, …, J; J is the number of neurons in this layer.) neuron, it receives the input signal x_i (i=1, 2, …, I; I is the number of neurons in the previous layer) whose weight is denoted as w_{ij}. Through "*tansig*" activation function, the output value calculated by the j^{th} neuron is expressed as

$$y_j = \frac{1-e^{-2\sum_{i=1}^{I} x_i w_{ij}}}{1+e^{-2\sum_{i=1}^{I} x_i w_{ij}}} \tag{6}$$

The loss function of MLP NN is

$$Loss = \frac{1}{MN}\sum_{m=1}^{M}\sum_{n=1}^{N}(f_{mn} - \hat{f}_{mn})^2 \tag{7}$$

where f_{ij} is the corrected exposure dose obtained through model-based PEC method; $\hat{f}_{ij}$ is the forward inference results after each optimization of MLP neuron weights.

The back propagation (BP) algorithm minimizes the loss function by repeatedly modifying the weights w_{ij}, and the correction factor Δw_{ij} of the weight w_{ij} is

$$\Delta w_{ij} = -\sigma\frac{\partial Loss}{\partial w_{ij}} \tag{8}$$

where $\frac{\partial Loss}{\partial w_{ij}}$ is the partial derivative of the loss function with respect to the weight on the neuron, which is following the chain derivation rule; σ is the learning rate. Each MLP training will correct the neuron weights of the entire network until the loss function is lower than the preset accuracy.

C. PEC with MLP NN

After introducing the traditional PEC method and the proposed MLP NN architecture, the MLP NN-based PEC method is as follows:

***Step* (1)** EBL process simulation. PSFs are simulated and fitted for the specified EBL process parameters. The calculated PSF represents the energy deposition distribution of electron beam scattering in this EBL process.

***Step* (2)** Sample generation. A series of equally spaced grating layouts with different periods are designed. Model-based PEC calculations are performed on these layouts by traditional dose-based PEC methods. Each original target layout is matched with the layout after PEC as MLP NN training samples. We further increase the diversity of the data set through processing methods such as flipping and translation.

***Step* (3)** MLP NN training. The energy deposition at a pixel of the photoresist is only related to the linear distance between this pixel and the exposure pixel. We divide the exposure pixel into l annular regions affected by a specific PSF. After establishing a fully connected MLP NN, a series of parameters are set such as the activation function of each layer, MLP NN training function, learning rate, and convergence conditions. Finally, we cyclically traverse each exposure pixel of all training layouts designed in *Step* (2) for MLP NN training.

***Step* (4)** MLP NN inference. We obtain the weights and biases of each trained neuron after *Step* (3) for MLP NN inference prediction. According to the data format of the MLP input layer, the layout to be corrected is calculated by the trained MLP NN inference, and the predicted dose after the PEC of each exposure point is obtained.

III. Result

This paper simulates 15keV e-beam exposure of 100 nm thick the polymeric methyl methacrylate (PMMA) resist on Si substrate. The parameters α, β, and η of the 2G PSF are 12.20 nm, 708.72 nm, and 1.15, respectively which are obtained by HNU-EBL software [12-14] (http://www.ebeam.com.cn).

The whole training process is carried out under MATLAB commercial software. The number of neurons in the input layer is set to 12. The hidden layer is composed of three layers of 50×20×10 neuron structure and the number of neurons in the output layer is 1. The training set of MLP NN is used for the grating layouts of different sizes and cycles. The train function of NN is "*trainscg*" function, and the activation function of each layer of NN is the "*tansig*" function.

We verify the performance of the proposed method compared to the PEC method in terms of accuracy and efficiency. As shown in Fig. 3, columns (a), (b), and (c) are the EBL process of direct exposure, model-based PEC exposure, and proposed PEC method exposure, respectively. From the development profile, both the model-based PEC method and the MLP NN method can obtain better development patterns compared to no PEC. The learning rate and convergence error are set to 0.1, 10^{-5}, respectively.

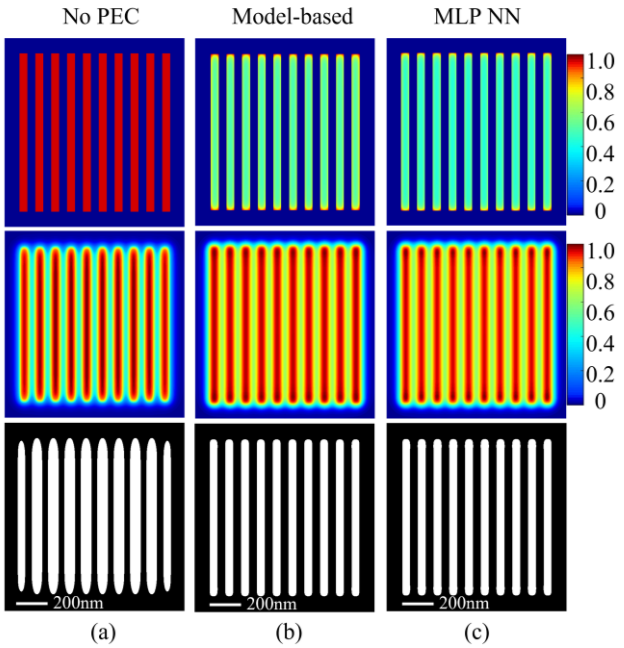

Fig. 3. Column (a) is the EBL process from exposure dose without PEC to developing contour for the grating structure with a 100 nm period. Columns (b) and (c) are the whole process like column (a) obtained by model-based PEC and MLP NN PEC methods respectively.

As shown in Fig. 4 (a), we design a series of grating comparison layouts with 40 nm width and 20 μm length. By adjusting the grating period T (from 120 nm to 280 nm), observe the changing trend of layout accuracy and efficiency. Obviously, as is shown in Fig. 4 (b), the development error obtained without PEC always maintains

a high level, which does not meet the requirements of experimental accuracy at all. The final development error (using Eq. (4)) obtained by the MLP NN inference can keep the same order of magnitude as the model-based PEC, generally less than 1%. As shown in Fig. 4 (c), for computational efficiency, the computational efficiency through MLP NN inference is 7~10 times higher than that of traditional model-based PEC. In the specified EBL process, the MLP NN model only needs to be trained once, so as to avoid repeating the complex model-based process.

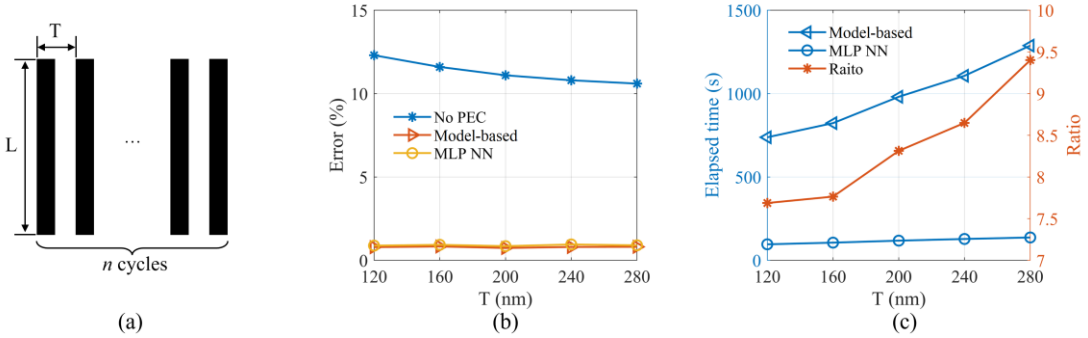

Fig. 4. (a) Schematic diagram of the designed grating comparison layout. (b) Comparison of final development errors under the three methods for different grating cycles. (c) Computational efficiency comparison between the proposed MLP method and the traditional model-based PEC method.

IV. CONCLUSION

This paper proposes an accurate and efficient PEC method for EBL based on MLP NN. According to the characteristics of the PSF, the exposure density of the annular region around the exposed pixels is used as the input, and the model-based PEC dose is used as the output. The trained network can directly obtain the final PEC dose through inference under a specific process model, avoiding computationally-expensive iterative calculations in conventional model-based PEC calculations. This article trains MLP NN based on the grating structure to verify the effectiveness of the proposed method. The PEC inference error of trained NN for grating with different periods can reach the same level as model-based PEC method (less than 1%), and the inference speed is more than 7~10 times faster than dose-based PEC.

ACKNOWLEDGMENT

This work is supported by the National Natural Science Foundation of China (#61804049); the Fundamental Research Funds for the Central Universities of P.R. China; Huxiang High Level Talent Gathering Project (#2019RS1023); the Key Research and Development Project of Hunan Province, P.R. China (#2019GK2071); the Technology Innovation and Entrepreneurship Funds of Hunan Province, P.R. China (#2019GK5029); the Fund for Distinguished Young Scholars of Changsha (#kq1905012); the National Natural Science Foundation of China (#62101182).

REFERENCES

[1] S. Liu, Z. Qu, Y. Fan, Y. Qi, L. Bai, W. Zhou, J. Lu, Y. Wang, and C. Han, "Multiscale fabrication of integrated photonic chips by electron beam lithography," in *10th International Symposium on Advanced Optical Manufacturing and Testing Technologies: Advanced and Extreme Micro-Nano Manufacturing Technologies*, 2021, vol. 12073, pp. 38-45: SPIE.

[2] H. Wei, D. Yunhui, Z. Lianqing, and D. Mingli, "Angular sensing system based on Y-type twin-core fiber and reflective varied-line spacing grating fabricated by electron beam lithography," *Results in Physics,* vol. 18, p. 103193, 2020.

[3] J. Zheng, J. Zhou, P. Zeng, Y. Liu, Y. Shen, W. Yao, Z. Chen, J. Wu, S. Xiong, Y. Chen, X. Shi, J. Liu, Y. Fu, and H. Duan, "30 GHz surface acoustic wave transducers with extremely high mass sensitivity," *Applied Physics Letters,* vol. 116, no. 12, p. 123502, 2020.

[4] W. Hu, Z. Qi, and H. Sun, "Design and fabrication of silicon-based optical phased array," in *AOPC 2021: Micro-optics and MOEMS*, 2021, vol. 12066, pp. 64-69: SPIE.

[5] T. Chang, "Proximity effect in electron - beam lithography," *Journal of vacuum science and technology,* vol. 12, no. 6, pp. 1271-1275, 1975.

[6] C.-H. Liu, P.-L. Tien, P. C. Ng, Y.-T. Shen, and K.-Y. Tsai, "Model-based proximity effect correction for electron-beam direct-write lithography," in *Alternative Lithographic Technologies II*, 2010, vol. 7637, p. 76371V: International Society for Optics and Photonics.

[7] J. J. Zarate and H. Pastoriza, "Correction algorithm for the proximity effect in e-beam lithography," in *2008 Argentine School of Micro-Nanoelectronics, Technology and Applications*, 2008, pp. 38-42: IEEE.

[8] R. C. Frye, E. A. Rietman, and K. D. Cummings, "Computation of proximity effect corrections in electron beam lithography by a neural network," in *1990 IJCNN International Joint Conference on Neural Networks*, 1990, pp. 7-14: IEEE.

[9] Y. Kwon, Y. Song, and Y. Shin, "Optical proximity correction using bidirectional recurrent neural network (BRNN)," in *Design-Process-Technology Co-optimization for Manufacturability XIII*, 2019, vol. 10962, pp. 68-75: SPIE.

[10] R. Luo, "Optical proximity correction using a multilayer perceptron neural network," *Journal of Optics,* vol. 15, no. 7, p. 075708, 2013.

[11] J. Zhou and X. Yang, "Monte Carlo simulation of process parameters in electron beam lithography for thick resist patterning," *Journal of Vacuum Science & Technology B: Microelectronics and Nanometer Structures Processing, Measurement, and Phenomena,* vol. 24, no. 3, pp. 1202-1209, 2006.

[12] W. Liu, W. Yao, C. Hou, H. Xu, H. Zhao, Y. Chen, H. Duan, and J. Liu, "HNU-EBL: A Software Toolkit for Electron Beam Lithography Simulation and Optimization," in *2021 International Workshop on Advanced Patterning Solutions (IWAPS)*, 2021, pp. 1-4: IEEE.

[13] C. Hou, W. Yao, W. Liu, Y. Chen, H. Duan, and J. Liu, "Ultrafast and Accurate Proximity Effect Correction of Large-Scale Electron Beam Lithography based on FMM and SaaS," in *2020 International Workshop on Advanced Patterning Solutions (IWAPS)*, 2020, pp. 1-3: IEEE.

[14] W. Yao, H. Zhao, C. Hou, W. Liu, H. Xu, X. Zhang, J. Xiao, and J. Liu, "Efficient Proximity Effect Correction Using Fast Multipole Method with Unequally Spaced Grid for Electron Beam Lithography," *IEEE Transactions on Computer-Aided Design of Integrated Circuits and Systems,* 2022.